Current Research in Pharmacology and Drug Discovery 3 (2022) 100100

Contents lists available at ScienceDirect

Current Research in Pharmacology and Drug Discovery

journal homepage: www.journals.elsevier.com/current-research-in-pharmacology-and-drug-discovery

Galantamine tethered hydrogel as a novel therapeutic target for streptozotocin-induced Alzheimer's disease in Wistar rats

Manickam Rajkumar [a], Murugesan Sakthivel [a], Kottaisamy Senthilkumar [b], Ramasundaram Thangaraj [c], Soundarapandian Kannan [a,*]

[a] Cancer Nanomedicine Laboratory, Department of Zoology, School of Life Sciences, Periyar University, Salem, 636 011, Tamil Nadu, India
[b] National Institute for Research in Tuberculosis/Indian Council for Medical Research, Ward No. 62, Government Rajaji Hospital Madurai, 625 001, Tamil Nadu, India
[c] Vermitechnology and Ecotoxicology Laboratory, Department of Zoology, School of Life Sciences, Periyar University, Salem, 636 011, Tamil Nadu, India

ARTICLE INFO

Keywords:
Alzheimer's disease
Acetylcholinesterase
Neuroinflammation
Gelatin methacrylate
Amyloid-β protein

ABSTRACT

Amyloid-β (Aβ) plaque formation, neuronal cell death, and cognitive impairment are the unique symptoms of Alzheimer's disease (AD). No single step remedy is available to treat AD, so the present study aimed to improve the drugability and minimize the abnormal behavioral and biochemical activities in streptozotocin (STZ) induced AD experimental Wistar rats. In particular, we explored the utilization of methacrylated gelatin (GelMA), which is a biopolymeric hydrogel that mimics the natural tissue environment. The synthesized biopolymeric gel contained the drug galantamine (Gal). Investigations were conducted to evaluate the behavioral activities of STZ-induced AD experimental rats under STZ + GelMA + Gal treatment. The experimental groups comprised the control and STZ, STZ + GelMA, STZ + Gal, and STZ + GelMA + Gal (10 mg/kg) treated rats. Intracerebroventricular STZ ensures cognitive decline in terms of an increase in the escape latency period, with a decrease in the spontaneous alteration of behavioral activities. Our results indicated decrease Aβ aggregation in the hydrogel-based drug treatment group and significant decreases in the levels of acetylcholinesterase and lipid peroxidation ($p < 0.001$). In addition, the glutathione and superoxide dismutase activities appeared to be improved in the STZ + GelMA + Gal group compared with the other treatment groups. Furthermore, histopathological and immunohistochemical experiments showed that the GelMA + Gal treated AD rats exhibited significantly improved behavioral and biochemical activities compared with the STZ treated AD rats. Therefore, STZ + GelMA + Gal administration from the pre-plaque stage may have a potential clinical application in the prevention of AD. Thus, we conclude that hydrogel-based Gal drugs are efficient at decreasing Aβ aggregation and improving the neuroinflammatory process, antioxidant activity, and neuronal growth.

1. Introduction

Alzheimer's disease (AD) is an inflammatory neurodegenerative disorder characterized by progressive cognitive decline, memory dysfunction, amyloid plaque formation, and synaptic and neuronal loss in the brain (Devi and Ohno, 2016; Fares et al., 2018). Pathophysiological changes in AD result in the extracellular accumulation of amyloid-β (Aβ) in plaques and the production of intracellular neurofibrillary tangles comprising hyperphosphorylated tau formations (Hahn et al., 2020; Garabadu and Verma, 2019). Aβ plaque formation is a major neuropathological hallmark of AD. In addition to the typical pathological changes in AD, oxidative stress is an important pathological phenomenon that manifests early in the course of AD, and that worsens AD pathology and cognitive dysfunction (Padurariu et al., 2010). The biochemistry of AD can be described by three different hypotheses comprising the amyloid hypothesis, cholinergic hypothesis, and tau hypothesis. Therefore, most AD treatment approaches are directed at the prevention or reversal of Aβ plaque formation (Nichol et al., 2010; Pierzynowska et al., 2019).

Oxidative stress is another hypothesis that has been implicated in the development of AD, where it causes mitochondrial and DNA damage. Excess Aβ aggregation and neuronal death is promoted by the accumulation of reactive oxygen species (ROS) as common pro-oxidative factors (Nichol et al., 2010; Pierzynowska et al., 2019). The oxidation states of brain peptides, lipids, and DNA are important oxidative stress markers that increase in AD (Takata et al., 2010; Canas et al., 2014). In addition, cognitive impairment is connected to cholinergic dysfunction, including

* Corresponding author.
E-mail address: skperiyaruniv@gmail.com (S. Kannan).

https://doi.org/10.1016/j.crphar.2022.100100
Received 10 November 2021; Received in revised form 5 April 2022; Accepted 13 April 2022

cholinergic neurons, neurotransmitters, and their receptors (Verreck et al., 2005; Halder et al., 2011). Oxidative stress appears to have a major role in AD and some studies suggest that Aβ neurotoxicity is linked to increases in acetylcholinesterase (AChE), lipid peroxidation (LPO), and ROS in the brain (Hahn et al., 2020; Watson et al., 2005).

Hydrogels are multi-functional polymeric materials with crosslinked hydrophilic networks. Gelatin is a natural polymer and it has been successfully applied in several nerve regeneration approaches (Jinhua et al., 2019). When combined with a conductive agent, hydrogels satisfy the necessary requirements to serve as ideal nerve conduits with flexibility, porosity, biocompatibility, biodegradability, neuro-inductivity, neuro-conductivity, and suitable surface and mechanical characteristics (Murugan et al., 2020; Mohamed et al., 2011; Nikkhah et al., 2012). However, gelatin is preferred due to its capacity to open epithelial junctions and permeate them. The good mechanical properties and superior transparency of these materials have led to their widespread use in surgical sutures, drug delivery systems, and tissue engineering (Hoch et al., 2012; Lin et al., 2013; Nipun Babu et al., 2019). In addition to its biological properties, gelatin has antibacterial, antioxidant, and targeting properties, as well as the capacity to regulate medication release (Billiet et al., 2014; Fares et al., 2018). Galantamine (Gal) is an alkaloid with disease-modifying effects via the stimulation of AChE inhibitors, and it has various functions such as neuroprotective effects, anti-inflammatory effects, and γ secretase activity suppression (Santos et al., 2002; Maelicke et al., 2001). Thus, Gal is an effective therapeutic management in memory impairment diseases such as AD (Hughes et al., 2010; Matharu et al., 2009). The drug Gal is widely applied because of its selective reversal of AD-induced symptoms/effects, including progressive cognitive decline and amyloid plaque formation.

In the present study, we applied hydrogel-tethered Gal to study its behavioral and biochemical effects on AD-induced rats. In particular, hydrogel-tethered Gal was applied to intracerebroventricular streptozotocin (ICV-STZ)-treated rats to assess its effects on their behavioral activities and biochemical parameters. We hypothesized that ICV-STZ treatment might enhance the formation of amyloid plaques and the tau pathology in experimental rats, thereby exacerbating their cognitive impairments. In particular, the neurotrophic/growth factor-mediated mechanism was investigated by assessing the neuropharmacological significance of methacrylated gelatin (GelMA) and Gal in the cortex and hippocampus based studies of the enzyme activities, Aβ protein expression, and behavioral and biochemical analyses in AD-induced rats.

2. Materials and methods

2.1. Animals

Male Wistar rat, (weighing 150–200 g) obtained from the Central Animal House facility at Periyar University, Salem, Tamil Nadu, India, were used in this study. Each live subject or subject group (n = 6 in each group investigated) was applied in various experiments. The experimental animals were kept under regulated photoperiodic conditions (12 h light/12 h dark cycle at a continuous temperature of 28 ± 2 °C and relative humidity (55%) in a controlled environment. Subjects were allowed free access to food and water. All experimental protocols were performed according to the guidelines of Committee for the Purpose of Control and Supervision of Experiments on Animals (CPCSEA), Government of India, and the experimental procedures were approved by the Institutional Animal Ethical Committee (PU/IAEC/2020/M1/14) of Periyar University, Salem, Tamil Nadu, India. Efforts were made to decrease distress in animals and the minimum number of animals was used in the experiments to ensure the statistical significance of the data.

2.2. Materials

STZ, gelatin (type A, 300 bloom from porcine skin), methacrylic anhydride (MA), and Gal were purchased from Sigma-Aldrich Company (Saint Louis, MO, USA). Sodium dodecyl sulfate (99%), oxidized glutathione, reduced glutathione (GSH), 2,4-dinitrophenylhydrazine, trichloroacetic acid, chloroform, ascorbic acid, ethylenediaminetetraacetic acid (EDTA), Tris buffer, and methanol were purchased from Himedia (India). Hydrogen peroxide (H_2O_2), bovine serum albumin (BSA), 5 5-dithiobis (2-nitrobenzoic acid), thiobarbituric acid (TBA), and reduced nicotinamide adenine dinucleotide were obtained from Sigma-Merck (India). Triton X-100, rabbit anti-Cx43 (1:500 dilution; Cell Signaling, USA), anti-Cx30 rabbit (1:500 dilution; Cell Signaling, USA), rabbit anti-PLC-gamma 1 antibody (1:100 dilution; Santa Cruz Biotechnology, USA), Anti-mGluR5 Antibody (1:100 dilution), Anti-Glial Fibrillary Acidic Protein antibody produced in rabbit (GFAP) (1:500 dilution), and Anti-NSE antibody produced in rabbit (1:100 dilution) were purchased from Sigma-Merck (India).

2.3. GelMA hydrogel synthesis

GelMA was synthesized as described previously (Fares et al., 2018; Annabi et al., 2014). Form type A gelatin at 10% (w/v) was mixed into Dulbecco's phosphate-buffered saline (PBS) at 40 °C and stirred until it is completely dissolved. MA was added to the gelatin solution under shaking at a temperature of 50 °C until it reached a rate of flow 0.5 mL/min, before then allowing the reaction to occur for 1 h. The fragment in the lysine group reaction was adjusted by modifying the MA value during the initial reaction of the compound. The mixture was diluted with distilled water, before diluting five times with more warm Dulbecco's PBS (40 °C) to extract salts, and reacting with methacrylic acid at 40 °C for one week using 12–14 kDa cut-off dialysis tubes. The compound was lyophilized for about 4 days to progress and obtain a pale white soluble spongy material, which was stored at −80 °C in a deep freezer until further use.

2.4. Administration of ICV-STZ

ICV-STZ injection was conducted as described previously according to the standard protocol (Kumar et al., 2016; Arora and Deshmukh, 2017). Briefly, each rat was anesthetized using ketamine hydrochloride (60 mg/kg i.p.). The coordinates for the lateral ventricle were correctly determined using the stereotaxic scale as 0.4 mm immediately below the cortex surface, 1.5 mm posterior to the suture in the sagittal plane, and 0.8 mm posterior to bregma. Before surgery, the solution (3 mg/kg) was freshly prepared by dissolving the STZ in artificial cerebrospinal fluid. A 28-gauge steel needle was connected to a 10-μL Hamilton syringe with a single-bilateral ICV injection tool (5 μL/ventricle) and the freshly prepared STZ solution was injected into the ICV-STZ group of rats. The control group underwent a similar surgical procedure but received 5 μL of normal saline.

2.5. Drugs and treatment schedule

The experimental rats were divided into five groups (six per group). The rats were anesthetized using general anesthesia (ketamine 60 mg/kg i.p) before drug treatment according to a previously described procedure (Grieb, 2016; Arora and Deshmukh, 2017). All of the hydrogel-based drug-treated animals were given a single daily dose using stereotactic apparatus (Table 1). Behavioral assessments were conducted during the treatment period with the Morris water maze (MWM), passive avoidance (PA), and Y-maze test (days 17–28). On the final day of the experiment, all rats were euthanized and their brains were surgically removed for biochemical, histopathological, and immunohistochemical studies (Fig. 1).

2.6. Body weight and blood glucose level

The weights of all the rats and their blood glucose levels were measured and recorded at intervals of 0, 7, 14, 21, and 28 days. At the

Table 1
Grouping of the experimental animals.

Group	Group name	Treatment
1	Control	Normal saline, surgery only performed
2	ICV-STZ	ICV- STZ (3 mg/kg/day; i.p) bilaterally administered
3	ICV-STZ + GelMA	GelMA (10 mg/kg/day; i.p.) administered to ICV-STZ + GelMA- injected rat
4	ICV-STZ + Gal	Gal (10 mg/kg/day; i.p.) administered to ICV-STZ + Gal injected rat
5	ICV-STZ + GelMA + Gal	GelMA + Gal (10 mg/kg/day; i.p.) administered to ICV-STZ + GelMA + Gal injected rat

start of the experiment before injection by ICV-STZ (day 0) and after the experiment on the final day (day 28), the body weights were estimated as described by Duelli et al. (1994) with the following formula:

Change in body weight = body weight on day 28 – body weight on day 0.

2.7. Behavioral assessments

2.7.1. MWM test

The MWM test is generally used to examine physical activity and spatial memory in a wide circular pool (Morris, 1984; Tuzcu and Baydas, 2006; Kumar et al., 2016). The MWM test was conducted in a circular pool (45 cm high and 150 cm in diameter, filled with water at a depth of 30 cm at a temperature of 28 ± 1 °C). Four equal quadrants were prepared in the tank (Q1–4), with a submerged platform (10 × 10 cm) in the center of the target quadrant at 1 cm below the water surface. The MWM test was performed for four consecutive days (days 17–20), where the animals completed four consecutive daily trials of training, each at approximately 30 min intervals (n = 6). The MWM was divided into three starting points marked by three equal platforms on the wall. A digital video camera recorded the locomotion activity of animals in several areas during the test and above the center of the MWM. For four days, each rat completed four training trials with three different starting locations every day (acquisition trial). During each trial of 30 s, rats were tested to determine whether they could find a hidden platform. After the platform elevated, the rats were allowed to stay on the platform for 30 s, before resting for 90 s. The rats that did not reach the platform were placed on it for 30 s. On the fourth day, probe testing was conducted to assess the improvement in spatial memory, where each rat was allowed 60 s of free-swimming time after the hidden platform was removed. The percentage of the escape latency time required to locate the hidden platform and time spent in the target quadrant were measured.

2.7.2. PA test

The PA step-through test is the most reliable method for assessing learning and cognitive functions in response to stress stimuli (Reeta et al., 2009). The unit comprised two similar boxes connected with a guillotine door (5 × 5 cm, and incandescent/dark 22 × 21 × 22 cm), and a steel shock grid foundation was present in the dark box. Before the experiment, the rat was given 60 s to become accustomed to the equipment. After 15 min, one rat was placed in a chamber with lights and the rat entered the dark box using the guillotine door. The time required by the rat to enter the darkroom was recorded as the initial retention delay (acquisition test). Any rat with an initial delay of more than 300 s was excluded from further trials. The door was closed after an electrical shock (0.5 mA, 50 Hz, 2 s once) and the rat that entered the darkroom remained on the floor grids for 300 s, before it was returned to its home cage. Between each exercise, the experimental boxes were cleaned to avoid confusion due to the presence of urine and fecal matter. After 24 h, the retention delay time was recorded for a maximum of 300 s in a similar manner to the previous test but without an electric shock. If the rat did not reach the darkroom box, a maximum delay of 300 s was recorded.

2.7.3. Y-Maze spontaneous replacement test

The Y-maze test was performed to assess the effectiveness of spontaneous replacement (spatial work memory) and locomotor function in the subjects used in the experiment (Wolf et al., 2016; Kitanaka et al., 2015). The Y-maze experiment used a maze with dimensions of 5 cm wide × 40 cm long × 15 cm high. The rats were kept in a maze box and permitted to freely move and select food. The number of entries in each arm of the maze was manually recorded and each rat participated in the maze experiment for 6 min. The alternative was defined as entry in all three arms in consecutive tests. The spontaneous alternation percentage was defined as the entry ratio for arm choices that varied from the selections relative to the total choices. The total number of arms entered per minute was then used to calculate the maximum number of spontaneous alternations, and the percentage was calculated as: actual alternations/maximum alternations × 100.

2.8. Biochemical measurements

2.8.1. Brain homogenate preparation

After completing the behavioral studies, ketamine hydrochloride (80 mg/kg, i.p.) was used to deeply anesthetize rats after the last experiment. All of the rats used in the study were then sacrificed and their brain tissues were immediately removed and cleaned with ice-cold saline (Ansab et al., 2019; Badruzzaman et al., 2012). The left and right cortex and hippocampus were dissected regionally and homogenized (10% w/v) in ice-cold PBS (0.1 M, pH 7.4). A centrifuge was used to separate

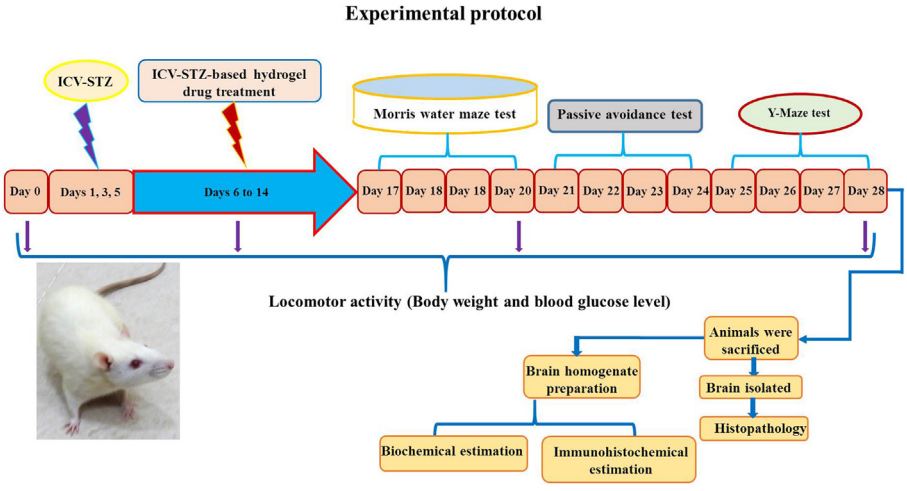

Fig. 1. Time schedule for drug administration procedure and group assignment: Rats were divided into 5 groups viz., control, and ICV-STZ, STZ + GelMA, STZ + Gal, STZ + GelMA + Gal treatment groups (n = 6). The sham control group received vehicle only. In ICV-STZ-treated groups, single ICV-STZ (3 mg/kg) injection was administered bilaterally to rats and other drug-treated groups (ICV-STZ, STZ + GelMA, STZ + Gal, and STZ + GelMA + Gal (10 mg/kg; i.p.)) were administered starting from the day after ICV-STZ administration for period of 1–14 days. The behavioral observations began on day 17, and the animals were sacrificed on day 28 following the ICV-STZ infusion after the behavioral examination to perform behavioural, biochemical, histopathological and immunohistochemical analysis.

the homogenate at 10,000×*g* and 4 °C for 15 min, and the supernatant was separated into aliquots for oxidative-nitrosamine biochemical assays (n = 4, total of six samples). The rat brain tissue was treated with 4% paraformaldehyde before histopathological examination, and with 10% sucrose followed by 20% sucrose in PBS at 4 °C before immunohistochemistry investigations. The protein concentration was determined in all samples using a protein assay kit (Thermo Scientific, USA).

2.8.2. Estimation of AChE activity

AChE activity (markers of cholinergic neurons in the brain) was assessed in the cortex and hippocampus as described previously (Ellman et al., 1961; Ansab et al., 2019). The mixture of Ellman's reagent contained 3 mL of sodium phosphate buffer (pH 8.0), 0.1 mL of acetylthiocholine iodide, 0.05 mL of supernatant, and 0.1 mL of DTNB (Ellman reagent) (0.01 M). The mixture was kept at 37 °C for 15 min until no further changes occurred. The absorption values were then recorded at 412 nm using an Ultraviolet–Visible (UV–Vis) spectrophotometer for 2 min at an interval of 30 s. The measurements were expressed as acetylthiocholine iodide micromoles of protein hydrolyzed/min/mg.

2.8.3. Determination of GSH content

The quantity of GSH was calculated using a previously described method with small modifications (Ellman et al., 1961; Jollow et al., 1974). Briefly, brain samples were mixed with 4.0% sulfosalicylic acid (w/v) at a ratio of 1:1 (v/v), incubated for 1 h at 4 °C, and then samples were immediately centrifuged at 4000×*g*, 4 °C for 10 min, before collecting the supernatant. Then, 0.1 mL of supernatant, 2.7 mL of PBS (0.1 M, pH 8.0), and 0.2 mL of 10 mM dithiobisnitrobenzoic acid was added, before incubating for 15 min and measuring the optical density at 412 nm. The results were calculated and expressed as μmol/min/mg of protein.

2.8.4. Superoxide dismutase (SOD) activity

The SOD activity was measured using the method described by Kakkar et al. (1984). The rat brain parts were homogenized in ice-cold 50 mM PBS (pH 7.0) containing 0.1 mM EDTA to obtain a 5% homogenate (w/v). The homogenates were centrifuged for 10 min at 10,000×*g* and 4 °C in a cooling centrifuge. The supernatant was separated and used for the enzyme assay. Approximately 100 μL of tissue homogenate was mixed with 880 μL of carbonate buffer (0.05 M, pH 10.2, containing 0.1 mM EDTA), before adding 20 μL of 30 mM epinephrine (in 0.05% acetic acid) to the mixture and measuring the optical density at 480 nm using an UV–Vis spectrophotometer. The SOD activity was expressed as the amount of enzyme that inhibited the oxidation of epinephrine by 50%, i.e., activity of unit/mg.

2.8.5. Catalase (CAT) activity

The CAT activity was evaluated by spectrophotometric analysis based on the rate of hydrogen peroxide decomposition (Aebi, 1984). An aliquot (5 μL) of each tissue supernatant was added (pH 7.0) to a cuvette containing 1.995 mL of 50 mM PBS. The reaction was initiated by adding 1.0 mL of freshly produced 30 mM H_2O_2 to the mixture. An UV–Vis spectrophotometer was used to measure the rate of H_2O_2 decomposition after 60 min at 240 nm. The CAT activity was expressed as the molar extinction coefficient for one unit activity equaling the number of moles of H_2O_2 destroyed per min/mg of protein.

2.8.6. LPO activity

The LPO activity was measured using a previously described method (Ramagiri and Taliyan, 2017; Ohkawa et al., 1979). The purple color produced by the interaction of MDA with TBA was measured spectrophotometrically. Briefly, 0.5 mL of tissue homogenate and 0.5 ml Tris-HCL were incubated at 37 °C for 2 h. The mixture combined with 1 ml of 10% trichloroacetic acid was added and centrifuged at 1000×*g* for 10 min. The mixture was then heated for 15 min in a hot water bath. After cooling to room temperature, the sample was centrifuged for 10 min at 3000×*g*. The sample was transferred to a test tube containing 2 mL of TBA solution and 1 mL of supernatant. Each tube was kept for 15 min in a hot bath water. The absorption of the sample was measured at 532 nm using an UV–Vis spectrophotometer. The MDA concentration was determined based on the expression of the TBA-MDA compound according to the absorption coefficient as protein μmol/min/mg.

2.9. Histopathological analysis

Standard procedures based on paraffin wax sectioning and hematoxylin–eosin staining was used for histological examinations (Schmued et al., 2008). The rats were anesthetized completely with ketamine hydrochloride (80 mg/kg i.p.) and then treated with 100 mL of cold PBS (PBS 0.1 m, pH 7.4) and 400 mL of a fixative solution containing 4% (w/v) paraformaldehyde in PBS. The brain was dissected and post-fixed overnight in the same buffer. The brain was washed in PBS for 1 h, dehydrated using a differential alcohol gradient, and finally implanted in paraffin wax. At the level of the hippocampus, sections with a thickness of 3 μm were removed, dewaxed, and stained with hematoxylin and eosin. Images were acquired with a light microscope (Olympus, BH-2) after processing the sections in DPX mounting solution.

2.10. Immunohistochemical analysis

Astrocytes or neurons were grown on glass coverslips after pretreatment with 10 mM poly-L-lysine (Sigma, USA). The cells were washed two times with warm PBS before fixing in 4% paraformaldehyde for 30 min (Tan et al., 2013). The cells were incubated in 0.3% Triton X-100 for 15 min, rinsed four times with PBS, and then incubated for 30 min with BSA. The cells were treated with the following antibodies overnight at 4 °C: rabbit anti-Cx43 (1:500 dilution; Cell Signaling, USA), rabbit anti-Cx30 (1:500 dilution; Cell Signaling, USA), rabbit anti-PLC-gamma 1 antibody (1:100 dilution; Santa Cruz Biotechnology, USA), rabbit anti-mGluR5 antibody (1:100 dilution; Santa Cruz Biotechnology, USA), rabbit anti-GFAP (1:500 dilution; Cell Signaling, USA), and Anti-NSE antibody produced in rabbit (1:100 dilution; Njjcbio, China). The cells were incubated with fluorescent secondary antibody rabbit IgG (Invitrogen, USA) for 1 h at room temperature on the next day, before rinsing four times and incubating with 4,6-Diamidine-2-phenylindole dihydrochloride (Beyotime, China) for 5 min. The cells were then washed four times and analyzed using a fluorescence microscope (Nikon Eclipse, Inc., Japan).

2.11. Protein estimation

Protein contents were estimated according to Lowry's procedure using BSA as a standard (Lowry et al., 1951).

2.12. Statistical analysis

GraphPad Prism (GraphPad Software, San Diego, CA, USA) was used to conduct all statistical analyses. The results were expressed as the mean ± standard deviation for n (number of animals examined) observations. Two-way analysis of variance (ANOVA) followed by Bonferroni's post hoc test for multiple comparisons were used to assess the learning behavior of rats. Biochemical data were evaluated by one-way ANOVA, followed by Tukey's test for multiple comparisons. In all experiments, $p < 0.05$ was considered to indicate a statistically significant difference.

3. Results

3.1. Behavioral assessments

3.1.1. Body weight and blood glucose level

The total body weights were recorded for the control group and other groups every 7 days (days 0, 7, 14, 21, and 28). A single bilateral

injection of ICV-STZ was applied in all groups except for the control group of animals. The animals in the treated groups had significantly lower body weights and higher blood glucose levels. Administration of STZ + GelMA, STZ + Gal, and STZ + GelMA + Gal (10 mg/kg) appeared to increase the body weight and reduce the blood glucose level when compared with the ICV-STZ treated group. Furthermore, the animals treated with STZ + GelMA + Gal (10 mg/kg) exhibited increased body weights and decreased blood glucose levels compared with the ICV-STZ group. The differences in the body weights ($F_{(4, 20)} = 6.583$, $R^2 = 0.5683$, $p < 0.0015$) and blood glucose levels ($F_{(4, 20)} = 4.048$, $R^2 = 0.4474$, $p < 0.0145$), among the experimental groups might have been due to the effects of the newly formulated hydrogel-based Gal, as shown in Fig. 2a and b (no significant change).

3.1.2. MWM test results

The MWM test was conducted to evaluate spatial memory improvements after ICV-STZ administration ($F_{(4, 15)} = 2.054$, $R^2 = 0.3539$, $p < 0.1380$). In the ICV-STZ group, the escape latency during the probe trial and in the target quadrant were dramatically improved on day 2 (151.87 ± 8.02%) and day 4 (121.54 ± 6.46%) compared with the control rats (87.77 ± 5.01%, and 43.94 ± 4.56%, respectively). During the probe trial, the escape latencies in the target quadrant were decreased in the group treated with STZ + GelMA (10 mg/kg) on day 2 (127.89 ± 6.38%), day 3 (103.55 ± 4.35%), and day 4 (91.80 ± 3.71%), as well as in the group treated with STZ + Gal (10 mg/kg) on day 2 (109.91 ± 7.32%), day 3 (90.80 ± 4.69%) and day 4 (76.92 ± 4.12%), and in the group treated with STZ + GelMA + Gal (10 mg/kg) on day 3 (88.54 ± 7.16%) compared with ICV-STZ-treated rats (151.87 ± 8.02%, 116.88 ± 6.00%, and 121.54 ± 6.46%, respectively). However, the escape delay for reaching the submerged site was significantly decreased in all experimental groups on the days of the MWM test and during the subsequent training days, and thus the behavioral activity of ICV-STZ-treated rats was undesirable. Finally, we found that the administration of hydrogel-based Gal drugs improved the behavioral activity of the ICV-STZ-treated rats (Fig. 3a).

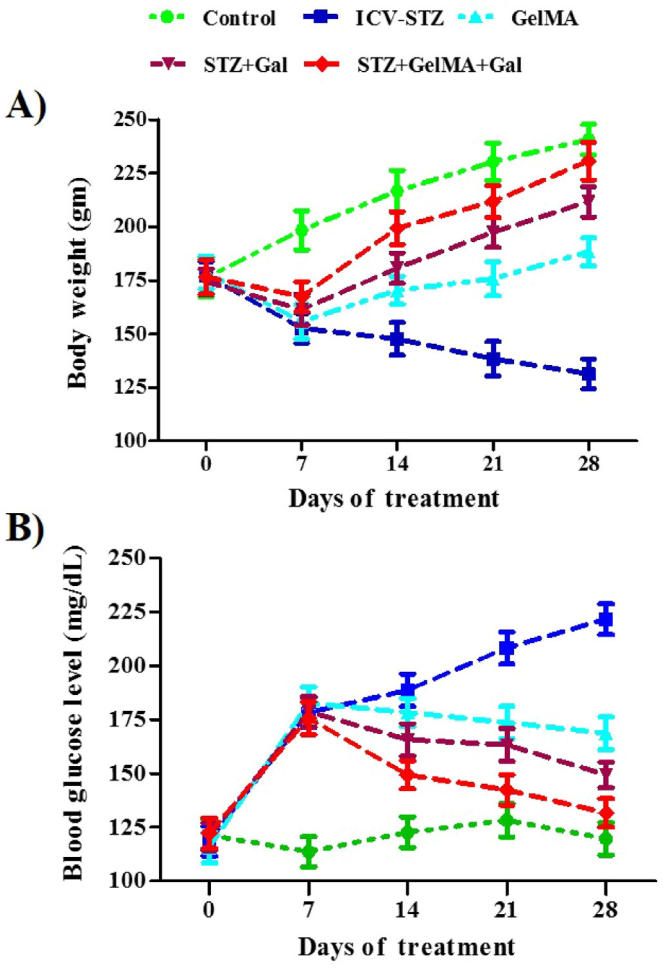

Fig. 2. Effect of hydrogel based drug loaded biomaterial on total body weight of control and experimental groups of rats (A). Effect of hydrogel-based drug loaded biomaterials on differences in the blood glucose level between control and experimental groups (B). Data presented as line diagram (mean ± SD). There is no significant difference with reference to body weight and blood glucose level (n = 6).

Following ICV-STZ administration, the MWM test was conducted to assess the time spent in the target quadrant on the experimental days, ($F_{(4, 15)} = 1.732$, $R^2 = 0.3159$, $p < 0.1954$). The ICV-STZ-treated group had difficulty remembering the location of the platform, as shown by their inability to recall the specific position of the platform, where they spent less time, appeared less frequently, and had a shorter total path length of time traversed in the target quadrant than the control group. The times spent in the target quadrant by the ICV-STZ-treated group were significantly lower on day 2 (48.81 ± 3.92%) and day 3 (63.81 ± 4.40%) compared with the control rats (90.94 ± 5.45% and 126.81 ± 6.14%, respectively). The times spent in the probe trial were significantly higher in the STZ + GelMA group (10 mg/kg) on day 3 (83.10 ± 3.65%) and day 4 (97.19 ± 6.03%), in the STZ + Gal group (10 mg/kg) on day 2 (77.11 ± 4.73%), day 3 (93.14 ± 5.23%), and day 4 (115.87 ± 5.73%), and in the STZ + GelMA + Gal group (10 mg/kg) on day 2 (89.14 ± 3.62%) and day 3 (113.54 ± 6.76%) compared with the ICV-STZ-treated rats (48.81 ± 3.92%, 63.81 ± 4.40%, and 74.67 ± 4.44%, respectively). However, in the STZ + GelMA + Gal group (10 mg/kg), the frequency of onset was higher and the time spent in the probe trial was greatly improved compared with the control and ICV-STZ-treated rats (Fig. 3b).

3.1.3. PA test results

Significant differences were observed among the control and experimental groups in the learning trials ($F_{(3, 16)} = 0.6575$, $R^2 = 0.1098$, $p < 0.5900$). The transfer latency was significantly decreased in the ICV-STZ group on day 2 (43.87 ± 2.79%) and day 3 (30.84 ± 2.24%) compared with the control rats (65.57 ± 3.89% and 75.84 ± 4.52%, respectively). The transfer latencies were found to be significantly increased in the STZ + GelMA group (10 mg/kg) on day 2 (63.60 ± 2.78%) and day 3 (60.97 ± 4.53%), in the STZ + Gal group (10 mg/kg) on day 2 (62.74 ± 3.62%) and day 3 (69.27 ± 2.01%), and in the STZ + GelMA + Gal group (10 mg/kg) on day 2 (65.50 ± 3.27%) and day 3 (68.47 ± 3.11%) compared with ICV-STZ-treated rats (43.87 ± 2.79% and 30.84 ± 2.24%, respectively). The hydrogel-based Gal drug-treated groups exhibited enhanced learning and memory when several shocks were applied to affect the transfer latency, thereby indicating that their learning and memory capacities were improved when compared with the control rats (Fig. 4a and b).

3.1.4. Y-Maze spontaneous alternation test results

The Y-maze spontaneous alternation test was conducted to examine whether the effects of ICV-STZ on learning and memory recovered under hydrogel-based Gal drug treatment in rats. The Y-maze spontaneous alternation occurred in the food intake test ($F_{(3, 16)} = 0.7473$, $R^2 = 0.1229$, $p < 0.5396$). The retention transfer latency was significantly increased in the ICV-STZ-treated rats on day 3 (61.94 ± 4.08%) compared with the control rats (24.57 ± 1.24%). The retention transfer latency was significantly reduced in the STZ + GelMA group (10 mg/kg) on day 2 (38.94 ± 2.09%) and day 4 (37.64 ± 1.51%), and in the STZ + Gal group (10 mg/kg) on day 2 (36.87 ± 3.76%) and day 3 (29.57 ± 3.17%) compared with ICV-STZ-treated rats (54.47 ± 3.31%, 61.94 ± 4.08%, and 70.54 ± 3.21%, respectively). The total arm entries did not vary and the dose of STZ + GelMA + Gal (10 mg/kg) administered appeared to decrease the error and enhance the memory function in the

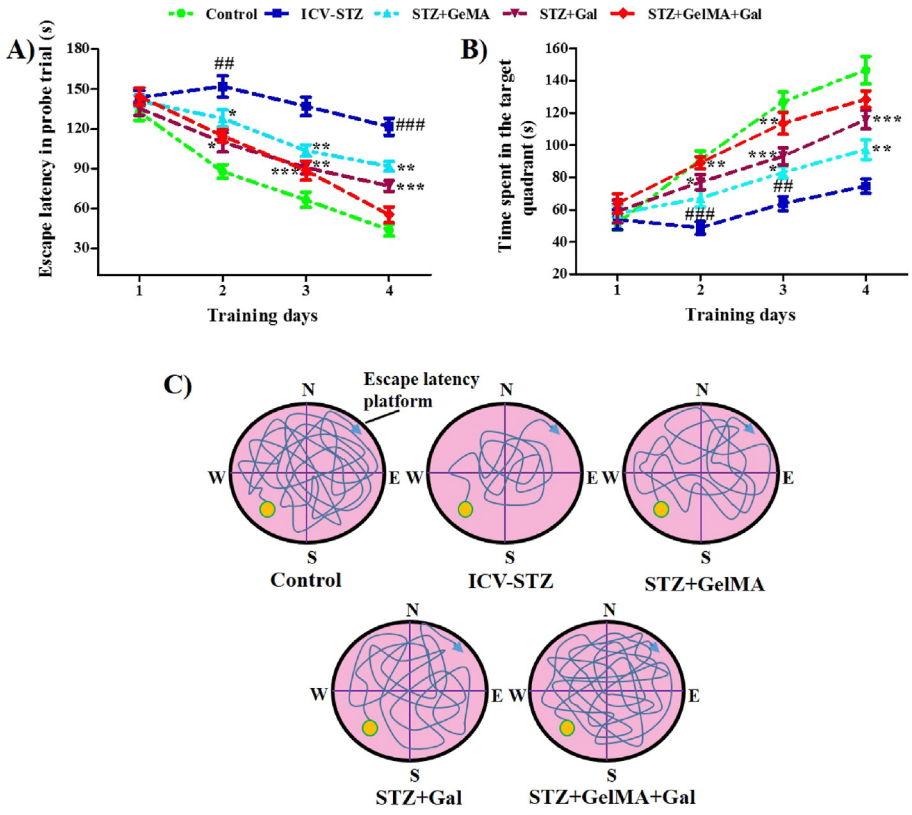

Fig. 3. Effect of hydrogel based drug loaded biomaterial on cognitive behavior of rats in MWM test and novel object recognition by ICV-STZ-injected in different experimental group of rats (n = 6). The learning curves for MWM acquisition trials across a period of 17–20 days are appreciable. The Rat were given four acquisition trials/day for two days using a visual platform and four days using an invisible platform, memory performance on escape latency and time spend in the probe trail between the control and experimental groups (A and B). MWM test for memory performance on time spent in target quadrant for the probe trail between the control and experimental groups of rats (C). Acquisition data is presented in line chart (mean ± SD) and it was analyzed by two-way ANOVA followed by Bonferroni's post hoc test for multiple comparisons. $^{\#\#}p < 0.01$, $^{\#\#\#}p < 0.001$ compared to control group and $^{*}p < 0.05$, $^{**}p < 0.01$, $^{***}p < 0.001$ compared to ICV-STZ group. *ICV-STZ* Intracerebroventricular Streptozotocin, *GelMA* Gelatin Methacrylate, *Gal* Galentamine.

experimental rats. However, the Y-maze test showed that hippocampal-dependent memory was more affected in ICV-STZ-treated rats because they spent less time on the new arm. The learning memory function was significantly improved in the hydrogel-based Gal drug-treated groups compared with the ICV-STZ treated rats (Fig. 4a and b).

3.2. Biochemical measurement

3.2.1. AChE activity levels

The effects of the treatments on the AChE activity in the cortex ($F_{(4, 25)} = 112.0$, $R^2 = 0.9472$, $p < 0.0001$) and hippocampus ($F_{(4, 25)} = 87.62$, $R^2 = 0.9334$, $p < 0.0001$) were investigated, as shown in Fig. 5a. ICV-STZ administration significantly increased the AChE levels in both the cortex (44.91 ± 3.13%) and hippocampus (51.53 ± 3.14%) brain supernatants compared with the control rats (19.87 ± 1.18% and 24.90 ± 2.14%, respectively). In addition, the AChE activity was significantly reduced in the STZ + Gal group (10 mg/kg) in the cortex (28.57 ± 2.90%) and STZ+GelMA and STZ+Gal (10mg/kg) group in the hippocampus (46.54 ± 3.83% and 34.93 ± 2.09%, respectively) compared with ICV-STZ-treated rats. Interestingly, the AChE activity was significantly decreased in the STZ + GelMA + Gal group (10 mg/kg) compared with ICV-STZ treated rats.

3.2.2. GSH activity levels

The effects of the treatments on the GSH activity in the cortex ($F_{(4, 25)} = 77.73$, $R^2 = 0.9256$, $p < 0.0001$) and hippocampus ($F_{(4, 25)} = 94.16$, $R^2 = 0.9378$, $p < 0.0001$) were investigated, as shown in Fig. 5b. ICV-STZ administered rats exhibited significantly decreased GSH levels in the hippocampus (31.53 ± 1.74%) compared with the control rats (62.61 ± 3.95%). The GSH levels were significantly increased in the cortex (33.90 ± 1.81%) in the STZ + GelMA group and in the hippocampus (50.60 ± 2.94%) in the STZ + Gal group (10 mg/kg) compared with ICV-STZ treated rats (24.57 ± 2.19 and 31.53 ± 1.74%, respectively). However, the GSH levels were restored in both the cortex and hippocampus in the STZ + GelMA + Gal group (10 mg/kg).

3.2.3. SOD activity levels

The effects of the treatments on the SOD activities in the cortex ($F_{(4, 25)} = 93.29$, $R^2 = 0.9372$, $p < 0.0001$) and hippocampus ($F_{(4, 25)} = 59.97$, $R^2 = 0.9056$, $p < 0.0001$) differed significantly, as shown in Fig. 5c. The SOD activity levels were significantly lower in the cortex and hippocampus (18.27 ± 2.59% and 21.20 ± 3.02) of the ICV-STZ treated rat brain supernatants compared with the control rats (39.61 ± 2.11% and 47.94 ± 2.71%, respectively). The SOD activity levels increased significantly in the cortex in the STZ + Gal group (26.87 ± 1.85%) and STZ + GelMA, and STZ + Gal groups (10 mg/kg) in the hippocampus (27.90 ± 2.86% and 35.91 ± 3.46%, respectively) compared with the ICV-STZ treated rats. However, no significant difference in the SOD activity was found between the STZ + GelMA + Gal group (10 mg/kg) rats compared with the ICV-STZ-treated rats.

3.2.4. CAT activity levels

The effects of the treatments on the CAT activity levels in the cortex ($F_{(4, 25)} = 42.81$, $R^2 = 0.8726$, $p < 0.0001$) and hippocampus ($F_{(4, 25)} = 36.26$, $R^2 = 0.8530$, $p < 0.0001$) differed significantly, as shown in Fig. 5d. The ICV-STZ treated rats had considerably reduced CAT activity levels in both the cortex and hippocampus (16.33 ± 1.07% and 25.66 ± 2.51%, respectively) as compared with the control rats (34.66 ± 2.78% and 43.66 ± 3.05%, respectively). In addition, administering STZ + GelMA (10 mg/kg) significantly increased the CAT level in the cortex (23.46 ± 1.98%), and in the hippocampus of STZ+GelMA and STZ + Gal (10 mg/kg) (32.76 ± 1.78% and 34.48 ± 2.08%, respectively) compared with ICV-STZ rats. In addition, the CAT activity levels in the cortex and hippocampus were higher in the STZ + GelMA + Gal group (10 mg/kg) than the ICV-STZ-treated rats.

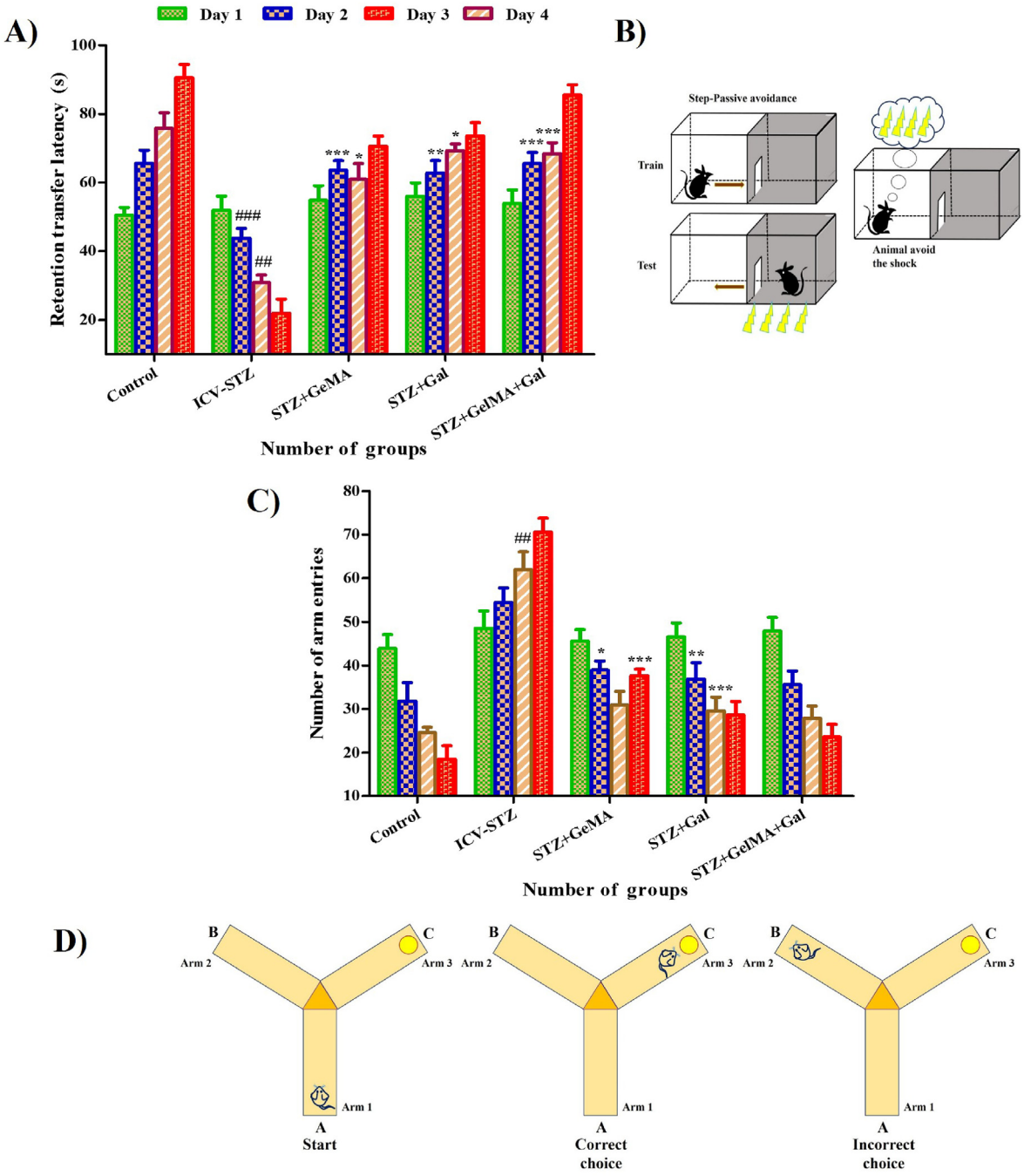

Fig. 4. Impact of hydrogel based drug loaded biomaterials on (n = 6) passive avoidance test for control and experimental groups of rats (A and B). Effect of hydrogel based drugs on retention transfer latency in Y maze test for control and experimental groups of rats (C and D). Acquisition data presented in bar chart was analyzed by two-way ANOVA followed by Bonferroni's post hoc test for multiple comparisons (mean ± SD). $^{\#\#}p < 0.01$, $^{\#\#\#}p < 0.001$ compared to control group and $^{*}p < 0.05$, $^{**}p < 0.01$, $^{***}p < 0.001$ compared to ICV-STZ group. *ICV-STZ* Intracerebroventricular Streptozotocin, *GelMA* Gelatin Methacrylate, *Gal* Galentamine.

3.2.5. *Effect on LPO activity*

The effects of the treatments on the LPO activity in cortex ($F_{(4, 25)} = 158.1$, $R^2 = 0.9620$, $p < 0.0001$) and hippocampus ($F_{(4, 25)} = 125.2$, $R^2 = 0.9524$, $p < 0.0001$) are shown in Fig. 5e. The ICV-STZ treated rats had significantly increased LPO levels in the hippocampus (142.90 ± 4.70%) compared with the control rats (89.81 ± 3.84%). The STZ + Gal (10 mg/kg) treatment significantly reduced the LPO level in the cortex (85.61 ± 5.75%) as compared with ICV-STZ rats (128.17 ± 3.74%). In addition, the LPO levels in STZ + GelMA and STZ + Gal (10 mg/kg) treated rats were significantly lower in the hippocampus (122.87 ± 6.18% and 115.61 ± 3.84%, respectively) compared with ICV-STZ-treated rats . The LPO level was greatly reduced in the STZ + GelMA + Gal group (10 mg/kg) compared with ICV-STZ-treated rats.

3.3. *Histopathological examination*

Histopathological analysis of the ICV-STZ group detected morphological changes in the neurons. Furthermore, ICV-STZ induced apoptosis in the neurons characterized by damaged neurons and amyloid plaque formation. The STZ + GelMA, STZ + Gal, and STZ + GelMA + Gal groups (10 mg/kg) exhibited reduced neuronal loss and amyloid plaque formation compared with ICV-STZ-treated rats. Surprisingly, the hydrogel-based drug

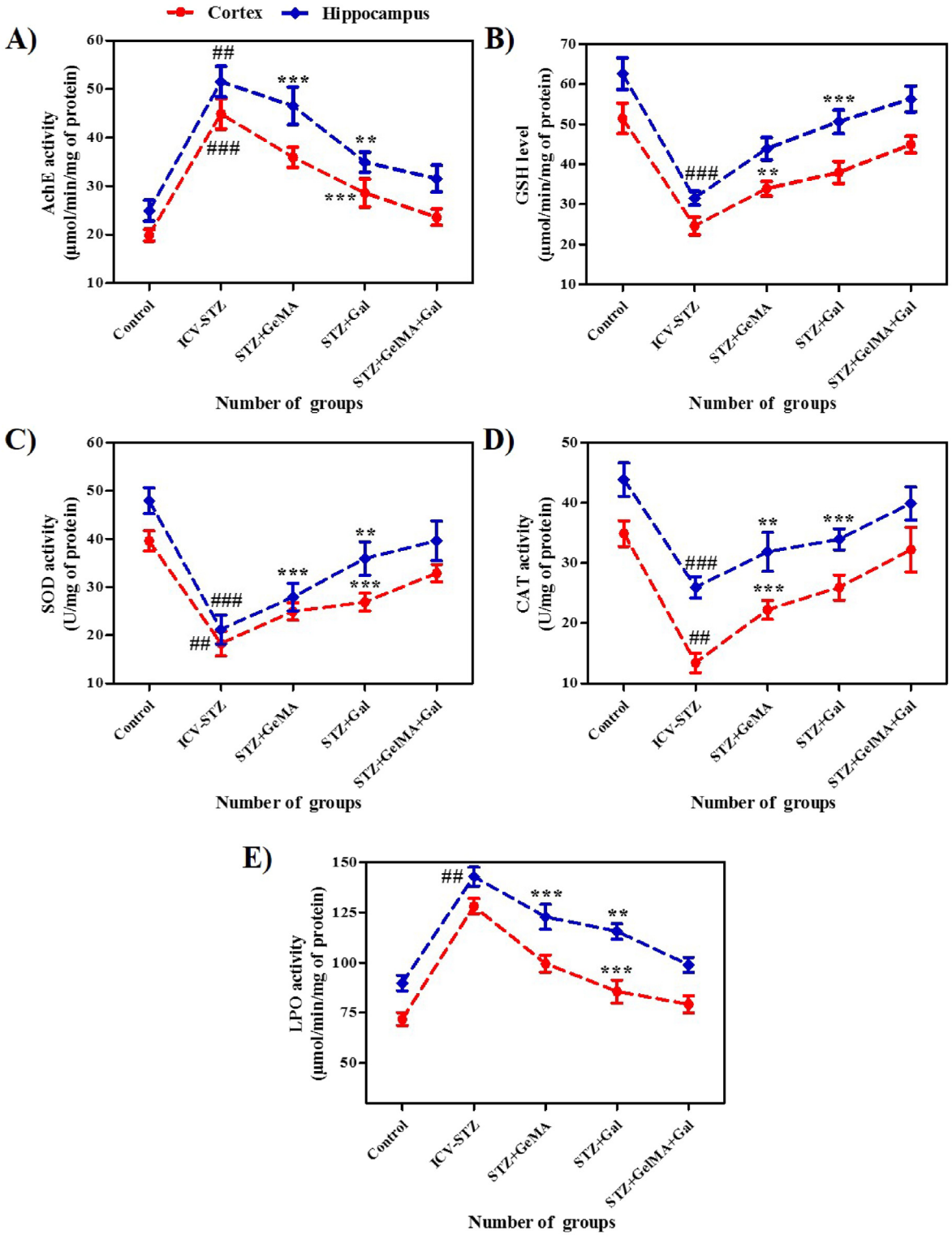

Fig. 5. The graphical representation revealed the enzymatic activity against hydrogel based drug loaded biomaterials in rats (A) AchE activity, (B) GSH activity, (C) SOD activity, (D) CAT activity, and (E) LPO activity in the cortex and hippocampus of control and ICV-STZ experimental groups of rats (n = 4). Acquisition data (mean ± SD), was analyzed by one-way ANOVA followed by Tukey's post hoc test for multiple comparisons and the data presented as line diagram (mean ± SD). $^{\#\#}p < 0.01$, $^{\#\#\#}p < 0.001$ compared to control group and $^{*}p < 0.05$, $^{**}p < 0.01$, $^{***}p < 0.001$ compared to ICV-STZ group. *ICV-STZ* Intracerebroventricular Streptozotocin, *GelMA* Gelatin Methacrylate, *Gal* Galentamine.

treatment groups had more healthy neurons with an oval shape and clear cytoplasm. In addition, the STZ + GelMA + Gal group (10 mg/kg) exhibited reduced amyloid plaque formation and improved neuronal cell growth compared with ICV-STZ-treated rats (Fig. 6a, b, 6c, 6d, and 6e).

3.4. Immunohistochemical analysis

Immunohistochemical analysis showed that ICV-STZ AD-induced neuronal apoptosis in the brains of ICV-STZ rats (Fig. 7a and b). STZ +

GelMA, STZ + Gal, and STZ + GelMA + Gal groups (10 mg/kg) as shown by the increased numbers of healthy neurons in their brains. No changes were observed in the ICV-STZ neuronal cells. These results demonstrate that hydrogel-based drug-treated neuronal cells and neuronal apoptosis were observed in the brains of ICV-STZ-treated rats. We also found decreased neuronal loss, increased number of healthy neurons, and higher levels of neuronal growth factor in the STZ + GelMA + Gal group (10 mg/kg).

4. Discussion

AD is an irreversible and progressive neurodegenerative disease, which results in deterioration of learning and memory, neuroprotective defects, and amyloid plaque formation in the brain. AD leads to imbalanced locomotion, behavioral dysfunction, and memory loss due to generation of free radicals (Mutlu et al., 2015; Butterfield et al., 2007). ICV-STZ induces the formation of free radicals and oxidative stress in part of the cortex and hippocampus in the brain, thereby causing significant learning and memory deficiencies due to brain damage in the cortex and hippocampus. There is evidence that ICV-STZ induces neuronal loss in the brain (Nichol et al., 2010; Pierzynowska et al., 2019).

In the present study, ICV-STZ caused prolonged impairment of glucose/energy metabolism, neuroinflammation, and oxidative stress in the brain, and finally learning and memory loss in rats (Oakley et al., 2006). The locomotor function did not differ significantly among the groups in this study which indicates that locomotion had no role in learning and memory (Ramagiri and Taliyan, 2017; Ansab et al., 2019). Furthermore, our results showed that the retention transfer latency changed significantly under ICV-STZ treatment due to impaired learning and memory as shown in previous studies (Pierzynowska et al., 2019; Ellman et al., 1961). We found changes in the locomotor function and body weight, and reduced blood glucose level under the hydrogel-based drug treatment Gal compared with ICV-STZ-treated rats (Demattos et al., 2012). These results indicate that hydrogel had positive effects on the body weight and control of the blood glucose level, which are key factors that affect the development of cognitive skills, such as memory and the learning efficiency in rats (Butterfield et al., 2007; Sachdeva and Chopra, 2015). Cognitive tests comprising MWM, PA, and Y-maze tests demonstrated that hydrogel-based Gal administration improved the behavioral and cognitive activities. The control-treated rats rapidly learned to swim in the MWM test during the acquisition phase. In the MWM test, rats treated with hydrogel-based drug performed better compared with ICV-STZ-treated rats (Garabadu and Verma, 2019; Zhang et al., 2012). The MWM test assesses spatial reference memory. The PA test assesses short-term memory impairment, which is known to occur earlier than spatial reference memory according to previous studies (Kumar et al., 2016; Sachdeva and Chopra, 2015). However, the Y-maze test based on the transfer latency for food intake showed that memory improvement occurred in the hydrogel-based drug treated rats compared with ICV-STZ induced rats, thereby indicating a greater effect on cognitive improvement (Wolf et al., 2016; Kitanaka et al., 2015).

The cholinergic distribution in parts of the brain, especially the hippocampus, plays important role in learning and memory. The single bilateral administration of ICV-STZ caused significant cognitive impairment, higher AchE concentration and LPO activity levels, and increased oxidative stress in the rat brain (Halder et al., 2011). However, the decline in cholinergic neuron cells was due to cholinergic hypofunction, which eventually led to cognitive impairment in ICV-STZ induced rats. Our findings strongly suggest that the hydrogel-based drug treatment affected LPO levels under oxidative stress, which is the phase before Aβ

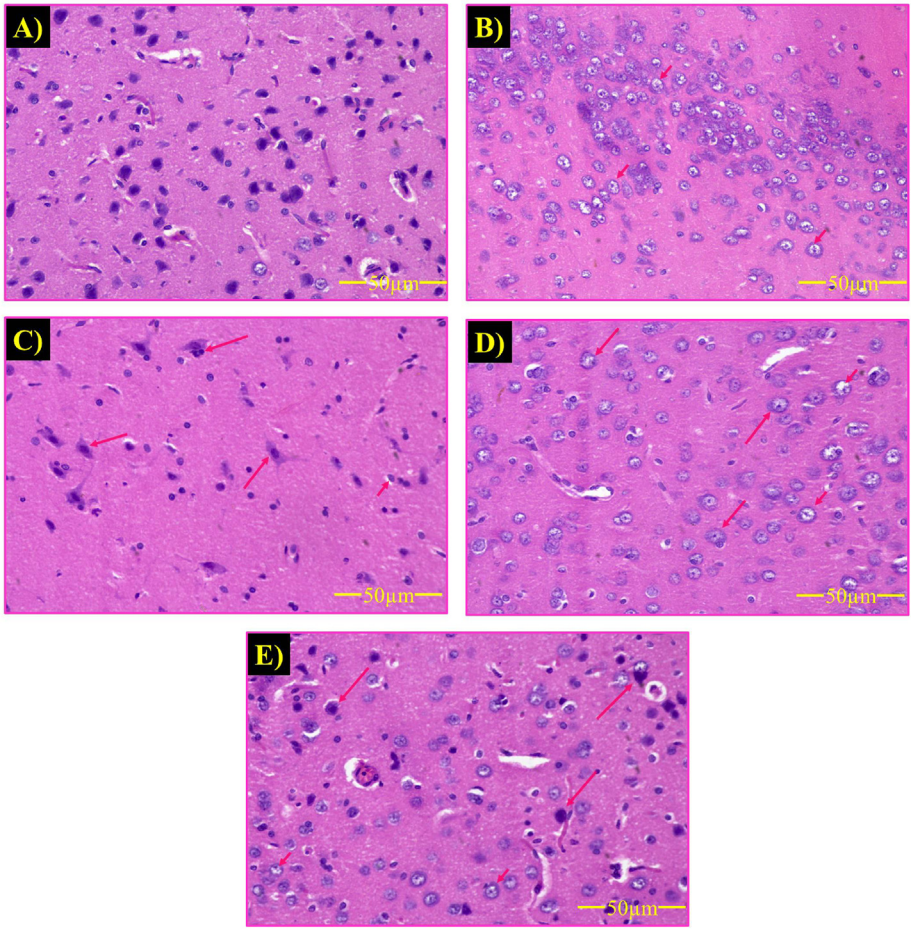

Fig. 6. Effect of hydrogel-based drug loaded biomaterial on histopathological changes in cerebral cortex of rats (n = 2). The photograph showed the neuronal damage of ICV-STZ-injected rats. ICV-STZ induced neuronal damage and cell apoptosis (short arrow). Vehicle-treated control group showing healthy neurons (A); ICV-STZ-treated group showing stained degenerated neurons (B); STZ + GelMA treated group (C); STZ + Gal treated group (D); STZ + GelMA + Gal treated group (E) revealed neuroprotection against ICV-STZ induced neurodegeneration. Glial cytoplasm blends with the neuropil, and dark nuclei often with a slight perinuclear halo. Cytologic preparation of normal cortex demonstrates normal oligodendrocytes, and astrocytes neurons (long arrow).

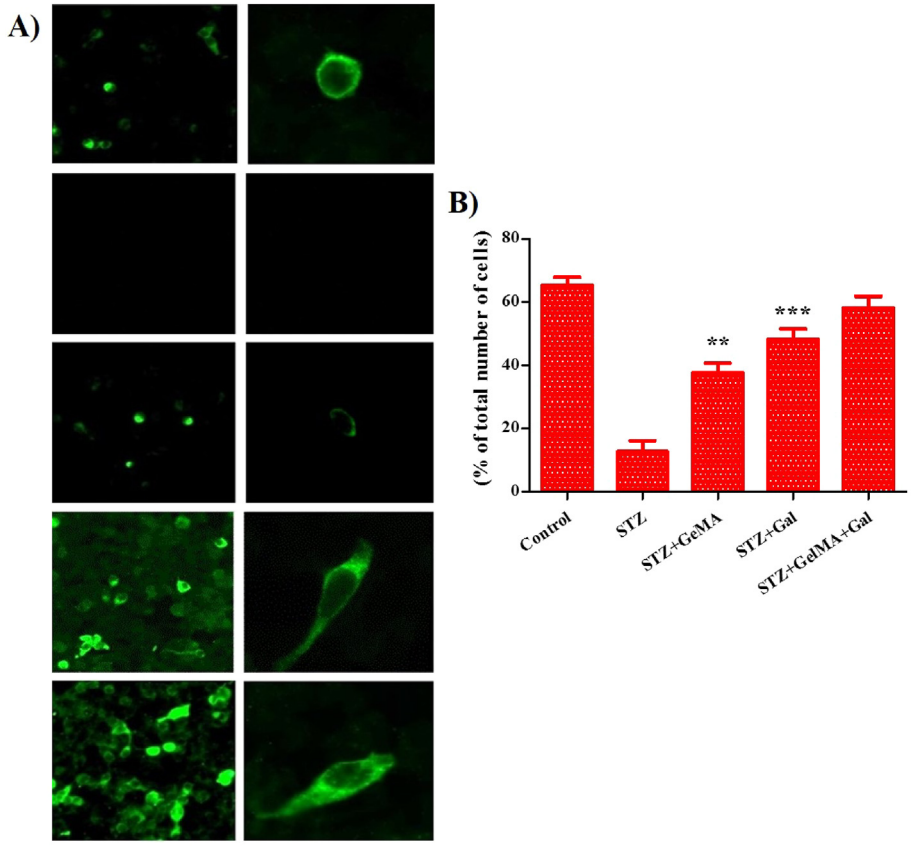

Fig. 7. Effect of hydrogel based drug loaded biomaterial proved its efficiency against the ICV-STZ injected rats as shown in fluorescence microscopic images (n = 2). The GSA-lectin in combination with thioflavin S staining revealed that the plaques were surrounded by reactive astrocytes and associated with activated microglia in ICV-STZ indicating neuroinflammation in brain nerve cells (A). Fluorescence image for different groups were subjected to Nissl staining to detect % of neuronal cells and Aβ protein expression in rats after drug treatment (B).

plaque appearance. Previous studies have shown that GSH decreases oxidative damage to the brain (Butterfield et al., 2007; Kumar et al., 2016). In the present study, treatment of the cortex and hippocampus was conducted because they are major parts of the brain involved in the pathogenesis of AD, and they are more susceptible to oxidative damage (Takata et al., 2010; Canas et al., 2014). Our findings are of therapeutic relevance because hydrogel-based Gal treatment can be applied as an effective combinatorial therapeutic strategy for improving cognitive functions. Increasing evidence indicates that the decreases in the activities of free radical scavenging enzymes, such as AchE, and in the LPO activity lead to the accumulation of free radicals such as H_2O_2. Our results suggest that GSH detoxified the free radicals generated in the brain and decreased H_2O_2 clearance compared with ICV-STZ-treated rats. The progression of oxidative stress in AD is associated with nuclear dysfunction, thereby leading to superoxide reduction and synaptic damage in ICV-STZ-treated rats according to previous studies (Hahn et al., 2020; Watson et al., 2005). Our hydrogel-based Gal treatment data complement previous observations of the SOD and CAT levels in rats. Our findings clearly demonstrate that the hydrogel-based drug treatment greatly increased the activities of GSH, SOD, and CAT, which have antioxidant activities. Thus, the hydrogel-based Gal treatment appeared to modulate the microglial function and enhance the clearance of Aβ to minimize neurotoxicity, and improve the redox state (Hoch et al., 2012).

Histological examinations of the control, hydrogel-based Gal drug treated, and ICV-STZ-treated rat brain parts detected very prominent nerve cells with a broad cortex region and many nuclei. According to previous studies, histopathological analyses detected high numbers of damaged neurons in parts of the brains of ICV-STZ treated rats, where the cells were wrinkled (Annabi et al., 2014; Pristera et al., 2013). On the last day of the experiment, the cortex and hippocampus regions contained neurotic plaques with focal, spherical, accumulations of dilated tortuous and dystrophic neurites, which were often located around a central amyloid plaque (Grayson et al., 2015; Sharma and Gupta, 2001). In the histological sections of AD-induced rats treated with STZ + GelMA, STZ + Gal, and STZ + GelMA + Gal (10 mg/kg), the numbers and sizes of the amyloid plaques were reduced, where focal gliosis was enhanced during the treatment period. In addition, the predominant neurodegenerative characteristics gradually decreased in AD-induced rats (Shin et al., 2012; Karran et al., 2011). Analysis of amyloid plaque samples from the cortex and hippocampus regions indicated lower amyloid plaque densities in the treated groups compared with the control group of rats, and this observation is in agreement with previous studies (Silva et al., 2014; Unger et al., 2006). Thus, the biomaterial formulation using the hydrogel-based Gal drug targeted specific parts of the brain.

Immunohistochemistry indicated that the hydrogel-based drug reduced the deposition of Aβ plaque rather than facilitating the clearance of existing deposits (Salomone et al., 2012). In agreement with this hypothesis, we observed clear signs of inflammation, antioxidant pressure, and apoptosis in plaque areas in the ICV-STZ-treated rats. As expected, immunostaining of the cells from hydrogel-based Gal treated rats detected surrounding positive plaques and cells positive for neurofibrillary tangles. A significantly high regulation of the proteins surrounding amyloid deposits was generally consistent with the inflammatory conditions comprising gliosis, inflammation, oxidative stress, and Aβ accumulation (Luikart et al., 2012; Roy et al., 2016). Immunohistochemistry supported the neuroprotective properties of the hydrogel-based Gal drug in the AD brain, and thus it is logical to conclude that it can prevent further damage caused by the deposition of plaques (Hoch et al., 2012; Sachdeva and Chopra, 2015).

In addition, the hydrogel-based Gal treatment modulated the microglial function to enhance Aβ clearance and suppress neurotoxic effects, with an improved redox state. Moreover, studies have shown that neurological diseases such as AD secondarily cause microglial senescence, which is connected with the loss of the microglial neuroprotective effect (Kumar et al., 2016; Matharu et al., 2009). In addition, neuroprotective pathways such as amyloid clearance and antioxidant activity

against AchE have been demonstrated effectively. However, as the disease progresses, increased oxidative stress causes excessive inflammation in ICV-STZ-treated rats (Oakley et al., 2006; Huang et al., 2015). The immobility of the inflammatory layer triggers a positive feedback process that results in the chronic loss of brain cells. In this context, our results support the possible use of hydrogel-based Gal administration to suppress the production of pro-inflammatory cytokines, improve the brain redox imbalance, and enhance spatial memory functioning (Hahn et al., 2020).

In this study, we evaluated oxidative stress in the brain and the memory impairment status based on behavioral and biochemical studies. Our results demonstrate that the hydrogel-based Gal treatment leads to improvement in the behavioral and biochemical activity levels. In addition, the AchE activity, LPO activity, and oxidative tissue damage were suppressed in ICV-STZ-treated rats when treated with the hydrogel-based Gal (Arora and Deshmukh, 2017). We assessed brain oxidative stress and the memory impairment status based on the behavioral and biochemical activity levels in hydrogel-based Gal treated rats (Ding et al., 2007; Canas et al., 2014). Unsurprisingly, the hydrogel-based Gal treatment effectively decreased Aβ aggregation.

Interestingly, our findings were supported by immunohistochemical analyses. Several other studies have emphasized the effects of neurological drugs on Aβ-plaque formation and deposition, where significant decreases in Aβ-plaque formation were reported. However, the most frequently used drugs have severe side effects and the prolonged use of these drugs does not affect the target sites in the brain, possibly due to increased drug resistance. In the present study, we used GelMA (hydrogel), which mimics the micro-environment of natural tissues and it allows the slow and steady release of the drug Gal in the brain, and this was evident at the histochemical level.

5. Conclusion

In this study, ICV-STZ-induced cognitive impairment in rats was treated with a hydrogel-based Gal drug, which is the best choice for treating AD. Increases in the AChE and LPO activity levels, hippocampal neuron loss, oxidative stress, and neuroinflammatory alteration occurred in the ICV-STZ treated rat brains. Behavioral studies indicated improved locomotor activity and memory enhancement under hydrogel-tethered Gal drug treatment, particularly the escape latency in the MWM and PA tests, compared with ICV-STZ treated rats. Thus, our results suggest that the reduced oxidative stress and cognitive-enhancing effects of hydrogel-tethered Gal drug treatment in the pre-plaque phase support its possible clinical application. In addition, histopathological and immunohistochemical analyses showed that hydrogel-based Gal drug treatment decreased Aβ accumulation and neuronal loss. Furthermore, hydrogel-based drugs that aim to enhance the neuro-inflammatory process, antioxidant activity, and neuronal growth factors could be studied effectively in this animal model of AD.

CRediT authorship contribution statement

Manickam Rajkumar: Investigation, Formal analysis, Methodology. **Murugesan Sakthivel:** Software, Formal analysis. **Kottaisamy Senthilkumar:** Investigation, Methodology, Data curation. **Ramasundaram Thangaraj:** Supervision, Data curation. **Soundarapandian Kannan:** Writing – review & editing, Supervision, Data curation.

Declaration of competing interest

The authors declare that they have no known competing financial interests or personal relationships that could have appeared to influence the work reported in this paper.

Acknowledgments

This study was financially supported through the University Research Fellowship (URF) from Periyar University, Salem-636011, Tamil Nadu, India (PU/AD-3/URF/013805/2019).

References

Aebi, H., 1984. Catalase in vitro. Methods Enzymol. 105, 121–126.
Annabi, N., Tamayol, A., Uquillas, J.A., Akbari, M., Bertassoni, L.E., Cha, C., 2014. 25th-anniversary article: rational design and applications of hydrogels in regenerative medicine. Adv. Mater. 26, 85–124.
Ansab, A., Jatinder, D., Priyanka, S., Ankit, U., Mahendra, B., Sangeeta, P.S., 2019. Chromium picolinate attenuates cognitive deficit in ICV-STZ rat paradigm of sporadic Alzheimer's-like dementia via targeting neuroinflammatory and IRS-1/PI3K/AKT/GSK-3β pathway. Inflammopharmacology.
Arora, R., Deshmukh, R., 2017. Embelin attenuates intracerebroventricular streptozotocin-induced behavioral, biochemical, and neurochemical abnormalities in rats. Mol. Neurobiol. 54 (9), 6670–6680.
Badruzzaman, M.K., Moshahid, M.K., Andleeb, K., Ejaz, A., Tauheed, I., Rizwana, T., Kumar, V., Ajmal, A., Fakhrul, I., 2012. Naringenin ameliorates Alzheimer's disease (AD)-type neurodegeneration with cognitive impairment (AD-TNDCI) caused by the intracerebroventricular-streptozotocin in rat model. Neurochem. Int. 61, 1081–1093.
Billiet, T., Gevaert, E., De Schryver, T., Cornelissen, M., Durrell, P., 2014. The 3D printing of gelatin methacrylamide cell-laden tissue-engineered constructs with high cell viability. Biomaterials 35, 49–62.
Butterfield, D.A., Reed, T., Newman, S.F., Sultana, R., 2007. Roles of amyloid beta-peptide associated oxidative stress and brain protein modifications in the pathogenesis of Alzheimer's disease and mild cognitive impairment. Free Radic. Biol. Med. 43, 658–677.
Canas, P.M., Simoes, A.P., Rodrigues, R.J., Cunha, R.A., 2014. Predominant loss of glutamatergic terminal markers in a β–amyloid peptide model of Alzheimer's disease. Neuropharmacology 76, 51–56.
Demattos, R.B., Lu, J., Tang, Y., Racke, M.M., Delong, C.A., 2012. A plaque-specific antibody clears existing β–amyloid plaques in Alzheimer's disease mice. Neuron 76, 908–920.
Devi, L., Ohno, M., 2016. Cognitive benefits of memantine in Alzheimer's 5XFAD model mice decline during advanced disease stages. Pharmacol. Biochem. Behav. 144, 60–66.
Ding, Q., Dimayuga, E., Keller, J.N., 2007. Oxidative damage, protein synthesis, and protein degradation in Alzheimer's disease. Curr. Alzheimer Res. 4, 73–79.
Duelli, R., Schrock, H., Kuschinsky, W., Hoyer, S., 1994. Intracerebroventricular injection of streptozotocin induces discrete local changes in cerebral glucose utilization in rats. Int. J. Dev. Neurosci. 12, 737–743.
Ellman, G.L., Lourtney, D.K., Andres, V., Gmelin, G., 1961. A new and rapid colorimetric determination of acetylcholinesterase activity. Biochem. Pharmacol. 7, 88–95.
Fares, M.M., Shirzaei Sani, E., Portillo Lara, R., Oliveira, R.B., Khademhosseini, A., Annabi, N., 2018. Interpenetrating network gelatin methacryloyl (GelMA) and pectin-g-PCL hydrogels with tunable properties for tissue engineering. Biomater. Sci. 6, 2938–2950.
Garabadu, D., Verma, J., 2019. Exendin-4 attenuates brain mitochondrial toxicity through PI3K/Aktdependent pathway in amyloid beta (1–42)-induced cognitive deficit rats. Neurochem. Int. 128, 39–49.
Grayson, B., Leger, M., Piercy, C., Adamson, L., Harte, M., Neill, J.C., 2015. Assessment of disease-related cognitive impairments using the novel object recognition (NOR) task in rodents. Behav. Brain Res. 285, 176–193.
Grieb, P., 2016. Intracerebroventricular streptozotocin injections as a model of Alzheimer's disease: in search of a relevant mechanism. Mol. Neurobiol. 53 (3), 1741–1752.
Hahn, B, Reneski, C.H, Lane, M, Elmer, G.I, Pereira, E.F.R, 2020. Evidence for positive allosteric modulation of cognitive-enhancing effects of nicotine by low-dose galantamine in rats. Pharmacol. Biochem. Behav. 199, 173043. In this issue.
Halder, S., Mehta, A.K., Kar, R., Mustafa, M., Mediratt, P.K., Sharma, K.K., 2011. Clove oil reverses learning and memory deficits in scopolamine-treated mice. Planta Med. 77, 830–834.
Hoch, E., Schuh, C., Hirth, T., Tovar, G.E.M., Borchers, K., 2012. Stiff gelatin hydrogels can be photochemically synthesized from low viscous gelatin solutions using molecularly functionalized gelatin with a high degree of methacrylation. J. Mater. Sci. Mater. Med. 23, 2607–2617.
Huang, T.T., Leu, D., Zou, Y., 2015. Oxidative stress and redox regulation on hippocampal-dependent cognitive functions. Arch. Biochem. Biophys. 576, 2–7.
Hughes, C.S., Postovit, L.M., Lajoie, G.A., 2010. Matrigel is a complex protein mixture required for optimal growth of cell culture. Proteomics 10, 1886–1890.
Jinhua, X., Yutong, L., Mohammad Ali, D., Genghong, T., Lu, H., Li, Y., Bin, X., Yue, W., Malcolm, X., Lin, Z., Lu, Z., 2019. An injectable conductive Gelatin-PANI hydrogel system serves as a promising carrier to deliver BMSCs for Parkinson's disease treatment. Mater. Sci. Eng. C (18), 31252–31259, 0928-493.
Jollow, D., Mitchell, J., Zampaglione, N.A., Gillette, J., 1974. Bromobenzene-induced liver necrosis. Protective role of glutathione and evidence for 3,4-bromobenzene oxide as the hepatotoxic metabolite. Pharmacol 11, 151–169.
Kakkar, P., Das, B., Viswanathan, P.N., 1984. A modified spectrophotometric assay of superoxide dismutase. Indian J. Biochem. Biophys. 21, 130–132.
Karran, E., Mercken, M., De Strooper, B., 2011. The amyloid cascade hypothesis for Alzheimer's disease: an appraisal for the development of therapeutics. Nat. Rev. Drug Discov. 10, 698–712.
Kitanaka, J., Kitanaka, N., Hall, F.S., Fujii, M., Goto, A., Kanda, Y., Koizumi, A., Kuroiwa, H., Mibayashi, S., Muranishi, Y., Otaki, S., Sumikawa, M., Tanaka, K., Nishiyama, N., Uhl, G.R., Takemura, M., 2015. Memory impairment and reduced

exploratory behavior in mice after administration of systemic morphine. J. Exp. Neurosci. 9, 27–35.
Kumar, A., Ekavali, Mishra, J., Chopra, K., Dhull, D.K., 2016. Possible role of P-glycoprotein in the neuroprotective mechanism of berberine in intracerebroventricular streptozotocin-induced cognitive dysfunction. Psychopharmacol. 233, 137–152.
Lin, R.Z., Chen, Y.C., Moreno-Luna, R., Khademhosseini, A., Melero–Martin, J.M., 2013. Transdermal regulation of vascular network bioengineering using a photopolymerizable methacrylated gelatin hydrogel. Biomaterials 34, 6785–6796.
Lowry, O.H., Rosebrough, N.J., Farr, A.L., Randall, R.J., 1951. Protein measurement with the folin phenol reagent. J. Biol. Chem. 193, 265–275.
Luikart, B.W., Perederiy, J.V., Westbrook, G.L., 2012. Dentate gyrus neurogenesis, integration, and microRNAs. Behav. Brain Res. 227, 348–355.
Maelicke, A., Samochocki, M., Jostock, R., Fehrenbacher, A., Ludwig, J., Albuquerque, E.X., Zerlin, M., 2001. Allosteric sensitization of nicotinic receptors by galantamine, a new treatment strategy for Alzheimer's disease. Biol. Psychiatr. 49, 279–288.
Matharu, B., Gibson, G., Parsons, R., Huckerby, T.N., Moore, S.A., 2009. Galantamine inhibits beta-amyloid aggregation and cytotoxicity. Neurol. Sci. J. 280, 49–58.
Mohamed, E.M., Ahmed, H.H., Estefan, S.F., Farrag, A.E.R.H., Salah, R.S., 2011. Windows into estradiol effects in Alzheimer's disease therapy. Eur. Rev. Med. Pharmacol. Sci. 15, 1131–1140.
Morris, R., 1984. Developments of a water-maze procedure for studying spatial learning in the rat. J. Neurosci. Methods 11 (1), 47–60.
Murugan, C., Rajkumar, M., Kanipandian, N., Thangaraj, R., Vimala, K., Kannan, S., 2020. Nanoformulated CPMSN biomaterial regulates proinflammatory cytokines to heal wounds and kills drug-resistant bacteria. Curr. Sci. 18 (10), 1583–1591.
Mutlu, O., Akar, F., Celikyurt, I.K., Tanyeri, P., Ulak, G., Erden, F., 2015. 7–NI and ODQ disturb memory in the elevated plus-maze, Morris water maze, and radial-arm maze tests in mice. Drug Target Insights 9, 1–8.
Nichol, J.W., Koshy, S.T., Bae, H., Hwang, C.M., Yamanlar, S., Khademhosseini, A., 2010. Cell-laden micro-engineered gelatin methacrylate hydrogels. Biomaterials 31, 5536–5544.
Nikkhah, M., Eshak, N., Zorlutuna, P., Annabi, N., Castello, M., Kim, K., et al., 2012. Directed endothelial cell morphogenesis in micropatterned gelatin methacrylate hydrogels. Biomaterials 33, 9009–9018.
Nipun Babu, V., Raju Vivek, R., Rejeeth, C., Kannan, S., 2019. Polymeric nanomaterial revolution in drug delivery systems: toward patient care. Mat. for Biomed. Eng. 33–58.
Oakley, H., Cole, S.L., Logan, S., Maus, E., Shao, P., 2006. Intraneuronal amyloid aggregates, neurodegeneration, and neuron loss in transgenic mice with five familial Alzheimer's disease mutations: potential factors in amyloid plaque formation. Neuroscience J. 26, 10129–10140.
Ohkawa, H., Ohishi, N., Yagi, K., 1979. Assay for lipid peroxides in animal tissues by the thiobarbituric acid reaction. Anal. Biochem. 95, 351–358.
Padurariu, M., Ciobica, A., Hritcu, L., Stoica, B., Bild, W., Stefanescu, C., 2010. Changes of some oxidative stress markers in the serum of patients with mild cognitive impairment and Alzheimer's disease. Neurosci. Lett. 469, 6–10.
Pierzynowska, K., Podlacha, M., Gaffke, L., Majkutewicz, I., Mantej, J., Węgrzyn, A., Osiadły, M., Myslinska, D., Węgrzyn, G., 2019. Autophagy-dependent mechanism of genistein-mediated elimination of behavioral and biochemical defects in the rat model of sporadic Alzheimer's disease. Neuropharmacology 148, 332–346.
Pristera, A., Saraulli, D., Farioli–Vecchioli, S., Strimpakos, G., Costanzi, M., Certo, M.G., 2013. Impact of N-tau on adult hippocampal neurogenesis, anxiety, and memory. Neurobiol. Aging 34, 2551–2563.
Ramagiri, S., Taliyan, R., 2017. Remote limb ischemic post conditioning during early reperfusion alleviates cerebral ischemic reperfusion injury via GSK-3β/CREB/BDNF pathway. Eur. J. Pharmacol. 803, 84–93.
Reeta, K.H., Mehla, J., Gupta, Y.K., 2009. Curcumin is protective against phenytoin–induced cognitive impairment and oxidative stress in rats. Brain Res. 1301, 52–60.
Roy, D.S., Arons, A., Mitchell, T.I., Pignatelli, M., Ryan, T.J., Tonegawa, S., 2016. Memory retrieval by activating engram cells in mouse models of early Alzheimer's disease. Nature 531, 508–512.
Sachdeva, A.K., Chopra, K., 2015. Naringin mitigate okadaic acidinduced cognitive impairment in an experimental paradigm of Alzheimer's disease. J. Funct.Foods 19, 110–125.
Salomone, S., Caraci, F., Leggio, G.M., Fedotova, J., Drago, F., 2012. New pharmacological strategies for the treatment of Alzheimer's disease: focus on disease-modifying drugs. Br. J. Clin. Pharmacol. 73, 504–517.
Santos, M.D., Alkondon, M., Pereira, E.F., Aracava, Y., Eisenberg, H.M., Maelicke, A., Albuquerque, E.X., 2002. The nicotinic allosteric potentiating ligand galantamine facilitates synaptic transmission in the mammalian central nervous system. Mol. Pharmacol. 61, 1222–1234.
Schmued, L., Bowyer, J., Cozart, M., Heard, D., Binienda, Z., Paule, M., 2008. Introducing Black Gold II, a highly soluble gold phosphate complex with several unique advantages for the histochemical localization of myelin. Brain Res. 1229, 210–217.
Sharma, M., Gupta, Y.K., 2001. Effect of chronic treatment of melatonin on learning, memory, and oxidative deficiencies induced by Intracerebroventricular streptozotocin in rats. Pharmacol. Biochem. Behav. 70, 325–331.
Shin, H., Olsen, B.D., Khademhosseini, A., 2012. The mechanical properties and cytotoxicity of cell-laden double–network hydrogels based on photocrosslinkable gelatin and gellan gum biomacromolecules. Biomaterials 33, 3143–3152.
Silva, R., Fabry, B., Boccaccini, A.R., 2014. Fibrous protein-based hydrogels for cell encapsulation. Biomaterials 35, 6727–6738.
Takata, K., Kitamura, Y., Saeki, M., Terada, M., Kagitani, S., Kitamura, R., Fujikawa, Y., Maelicke, A., Tomimoto, H., Taniguchi, T., Shimohama, S., 2010. Galantamine-induced amyloid-{beta} clearance mediated via stimulation of microglial nicotinic acetylcholine receptors. J. Biol. Chem. 285, 40180–40191.
Tan, G., Zhou, L., Ning, C., Tan, Y., Ni, G., Liao, J., 2013. Biomimetically–mineralized composite coatings on titanium functionalized with gelatin methacrylate hydrogels. Appl. Surf. Sci. 279, 293–299.
Tuzcu, M., Baydas, G., 2006. Effect of melatonin and vitamin E on diabetes-induced learning and memory impairment in rats. Eur. J. Pharmacol. 537, 106–110.
Unger, C., Svedberg, M.M., Yu, W.F., Hedberg, M.M., Nordberg, A., 2006. Effect of subchronic treatment of memantine, galantamine, and nicotine in the brain of Tg2576 (APPswe) transgenic mice. Pharmacol. J. Exp. Ther. 317, 30–36.
Verreck, G., Chun, I., Li, Y., Kataria, R., Zhang, Q., Rosenblatt, J., Decorte, A., Heymans, K., Adriaensen, J., Bruining, M., Van Remoortere, M., Borghys, H., Meert, T., Peeters, J., Brewster, M.E., 2005. Preparation and physicochemical characterization of biodegradable nerve guides containing the nerve growth agent sabeluzole. Biomat 26, 1307–1315.
Watson, D., Castano, E., Kokjohu, T.A., Kuo, Y.M., Lyubchenko, Y., Pinsky, D., Connolhy, E.S., Jr Esh, C., Luehrs, D.C., Stine, W.B., Rowse, L.M., Emerling, M.R., Roher, A.E., 2005. Physicochemical characteristics of soluble oligomeric Abeta and their pathologic role in Alzheimer's disease. Neurol. Res. 27, 869–881.
Wolf, A., Bauer, B., Abner, E.L., Ashkenazy-Frolinger, T., Hartz, A.M.S., 2016. A comprehensive behavioral test battery to assess learning and memory in 129S6/Tg2576 mice. PLoS One 11 (1), 0147733– 0147733.
Zhang, R., Xue, G., Wang, S., Zhang, L., Shi, C., Xie, X., 2012. Novel object recognition as a facile behavior test for evaluating drug effects in Abeta APP/PS1 Alzheimer's disease mouse model. J. Alzheim. Dis. 31, 801–812.